Different Effects of Iron Uptake and Release by Phytoferritin on Starch Granules

ARTICLE *in* JOURNAL OF AGRICULTURAL AND FOOD CHEMISTRY · AUGUST 2013

Impact Factor: 2.91 · DOI: 10.1021/jf402826p · Source: PubMed

5 AUTHORS, INCLUDING:

Tuo Zhang

Michigan State University

14 PUBLICATIONS **94** CITATIONS

SEE PROFILE

Liao Xiayun

China Agricultural University

9 PUBLICATIONS **74** CITATIONS

SEE PROFILE

Xu Chuanshan

The Chinese University of Hong Kong

69 PUBLICATIONS **508** CITATIONS

SEE PROFILE

Guanghua Zhao

China Agricultural University

128 PUBLICATIONS **2,030** CITATIONS

SEE PROFILE

JOURNAL OF AGRICULTURAL AND FOOD CHEMISTRY

Article

pubs.acs.org/JAFC

Different Effects of Iron Uptake and Release by Phytoferritin on Starch Granules

Tuo Zhang,[†] Xiayun Liao,[†] Rui Yang,[†] Chuanshan Xu,[‡] and Guanghua Zhao*[,†]

[†]CAU and ACC Joint-Laboratory of Space Food, College of Food Science and Nutritional Engineering, China Agricultural University, Beijing Key Laboratory of Functional Food from Plant Resources, Beijing 100083, China

[‡]School of Chinese Medicine, Chinese University of Hong Kong, Hong Kong, China

ABSTRACT: Phytoferritin from legume seeds is naturally compartmentalized in amyloplasts, where iron is takem up and released by ferritin during seed formation and germination. However, the effect of these two processes on starch granules remains unknown. No starch damage was visualized by SEM during iron uptake by apo soybean seed ferritin (SSF). In contrast, great damage was observed with the starch granules during iron release from holoSSF induced by ascorbic acid. Such a difference stems from different strategies to control $HO^{\bullet}$ chemistry during these two processes. $HO^{\bullet}$ is hardly formed during iron uptake by apoSSF, whereas a significant amount of $HO^{\bullet}$ is generated during iron release due to the Fenton reaction. As a result, starch granules are kept intact during iron uptake, which might beneficial to the storage of the starch granules during seed formation. In contrast, these starch granules are dramatically hydrolyzed during the iron release process, which might favor seed germination.

KEYWORDS: *phytoferritin, starch granules, amyloplast, hydroxyl radical, hydrolysis, ascorbic acid*

INTRODUCTION

Iron homeostasis in various plant tissues throughout the life cycle is a dynamic process resulting from an integrated regulation of the expression of various genes encoding proteins acting in the transport, storage, and utilization of iron.[1,2] When iron is allowed to redox cycle (e.g., as in cytochromes or peroxidases), it contributes to activation of reduced forms of oxygen through Fenton chemistry, leading to cellular damage and possibly cell death. One of the most commonly accepted mechanisms by which iron is involved in free radical production in vivo is demonstrated by the iron-participated Fenton reaction.[3,4]

The hydroxyl radical ($HO^{\bullet}$) is a potent oxidant that reacts at diffusion-limited rates (10^8–10^9 M^{-1} s^{-1}) with almost every type of molecule found in living cells including sugars, amino acids, nucleic acids, lipids, and organic acids.[5,6] In contrast, $HO^{\bullet}$ was also reported to play a positive role in several physiological processes such as plant cell-wall loosening for the control of elongation growth[7] and protection of the emerging seedling against pathogen attack.[8] Therefore, it is of great importance for living organisms to regulate iron-related hydroxyl radical chemistry.

Ferritin is a specific class of iron storage protein, which is implicated in the buffering and transit of iron. Ferritin was found in the entire living kingdom except for yeast.[9] Subunit analyses indicate that animal ferritin is composed of two types of subunits, designated H and L, which coassemble in different ratios to form a protein shell of 24 subunits. These H and L subunits share 55% identity in amino acid sequences and similar three-dimensional structures with each other. The H-chain subunit has ferroxidase activity associated with a di-iron binding center that is responsible for the rapid oxidation of Fe^{2+} to Fe^{3+} by O_2 or H_2O_2, whereas the L-chain subunit appears to provide efficient sites for iron nucleation and mineralization.[10,11]

Iron uptake by ferritin corresponds to iron storage, which has been extensively studied recently.[9] The di-iron ferroxidase center plays a key role in this process, but its role becomes less important when iron cores are formed within the inner cavity of the protein. By then, most iron ions are oxidized and deposited directly on the surface of the mineral cores through the crystal growth model.[12] The major cellular oxidants consumed during this oxidation reaction are oxygen and hydrogen peroxide.[13] Sequestered ferric iron is bioavailable in case of cellular needs and is nonreactive with oxygen. In contrast to the above iron storage, there are relatively fewer studies carried out with iron release from ferritin, especially from phytoferritin.[14] The iron release is of crucial importance because this process is involved in cell growth both in plants and in animals. Phytoferritin iron from legume seeds is required for the germination and early growth of seedlings.[15] However, the mechanism by which phytoferritin regulates its iron complement to the physiological process remains unknown.

Compared with animal ferritin, phytoferritin exhibits distinctive structural and functional features. One major difference is that phytoferritin occurs in plastids where iron is incorporated into the ferritin shell to form the mineral core, whereas animal ferritin occurs in the cellular cytoplasm. For example, phytoferritin in seeds was located in amyloplasts, where starch granules were synthesized and stored.[16,17] It has been reported that during iron uptake, reactive oxygen species (ROS) including H_2O_2 and $HO^{\bullet}$ are produced as byproducts in the presence of animal ferritin.[18,19] On the other hand, $HO^{\bullet}$ was also produced during iron release from holo pea seed ferritin in the presence of ascorbic acid.[20] A model based on the

Received: April 15, 2013
Revised: August 2, 2013
Accepted: August 2, 2013
Published: August 2, 2013

observation that the immunodetection pattern of pea seedling ferritin is similar to the pattern of ferritin degraded by free radical during in vitro iron exchanges has been proposed.[21] It has been hypothesized that such a mechanism occurs during seed germination.[21] Because starch granules coexist with phytoferritin in the amyloplasts of seeds, it is of special interest to elucidate whether these two processes (iron uptake and release) have effects on starch granules, the focus of this study.

Herein, we demonstrated that iron uptake and release by plant ferritin have different effects on starch granules due to their different strategies for hydroxyl radical chemistry. $HO^{\bullet}$ was hardly detected during iron uptake by apoferritin. Because this iron uptake process mainly occurs during seed formation, it might be beneficial to the formation and growth of starch granules. In contrast, a significant amount of $HO^{\bullet}$ was generated during iron release from ferritin, resulting in the hydrolysis of starch granules to a great extent, facilitating the generation of reducing sugars, which may favor seedling growth.

MATERIALS AND METHODS

Materials. Dried soybean (*Glycine max*) seeds were obtained from the local market. The ferrous iron chelator 3-(2-pyridyl)-5,6-bis(4-phenylsulfonic acid)-1,2,4-triazine (ferrozine) was obtained from Sigma-Aldrich Chemical Co. (Shanghai, China). Sephacryl S-300, DEAE Sepharose Fast Flow, native electrophoresis marker, and SDS electrophoresis marker were purchased from GE Healthcare Bio-Sciences AB (Beijing, China). 3-(*N*-Morpholino)propanesulfonic acid (Mops) was obtained from Amersco (Beijing, China). Ascorbic acid, terephthalic acid (TA), mannitol, thiourea, sodium citrate, and magnesium chloride hexahydrate were obtained from Beijing Chemical Reagents Co. (Beijing, China). All other reagents used were of analytical grade or purer. HoloSSF and apoSSF were prepared as previously described.[22−24] Antiferritin rabbit antiserum was purchased from Beijing Protein Institute. Protein concentrations were determined according to the Lowry method with BSA as standard.

Subcellular Localization of SSF. The samples were prepared according to a reported method.[25,26] After 12 h of imbibition, soybean seeds were cut into small patches. The patches were perfused with 4% paraformaldehyde and 2.5% glutaraldehyde in 100 mM PBS. They were dehydrated in a graded ethanol series and embedded in Epon. Ultrathin sections of the specimens were cut and treated for 10 min with 35 mM glycine, after which they were immersed with PBS buffer containing 5% BSA and then incubated overnight at 4 °C with antiferritin rabbit antiserum (1:500). Next they were incubated with immunogold-conjugated goat anti-rabbit secondary antibody (Jackson Immuno Research Laboratories, Inc., West Grove, PA, USA; dilution, 1:20), after which the sections were stained with neutral uranyl acetate for 5 min. The samples were examined in a New Bio-TEM H-7500 transmission electron microscope (Hitachi Ltd., Japan).

Kinetic Measurement of Iron Uptake. Iron uptake by apoSSF was investigated using the reported procedure.[27] The fast kinetic experiment was undertaken with the pneumatic drive Hi-Tech SFA-20 M stopped-flow accessory on a Varian Cary 50 spectrophotometer (Varian, USA). Equal 140 μL volumes of weakly acidic $FeSO_4$ solution and buffered apoferritin solution were mixed at 25 °C in the thermostated sample compartment containing a 280 μL quartz stopped-flow cuvette with 1 cm optical path length. μ-Oxo-diFe^{3+} species were formed during iron uptake, which were monitored by 300 nm.

Kinetic Measurement of Iron Release. Iron release from holoSSF was investigated by the reported method.[22,28] Briefly, the assay system (1 mL) contained 0.2 μM holoSSF, 500 μM ferrozine, 100 mM NaCl, and the desired concentration of ascorbic acid in 50 mM Mops buffer, pH 7.0. Reactions were carried out at 25 °C against reference cuvettes containing all reactants and were initiated by the addition of ascorbic acid. The development of $[Fe(ferrozine)_3]^{2+}$ was measured by recording the increase in absorbance at 562 nm using a Varian Cary 50 spectrophotometer and the iron released estimated, using ε_{562} = 27.9 mM^{-1} cm^{-1}. The kinetic data were further analyzed with Origin 8.0 software (Microcal Inc.). The initial rate (ν_0) of iron release measured as Fe^{2+}−ferrozine complex formation was obtained from the linear A_1 term of third-order polynomial fitted to the experimental data as described previously: namely, $Y = A_0 + A_1t + A_2t^2 + A_3t^3$ and $dY/dt = A_1 + 2A_2t + 3A_3t^2$ (at t = 0, $(dY/dt)_0 = \nu_0$). Here t is the time in seconds and Y is the concentration of $[Fe(ferrozine)_3]^{2+}$ at time t in seconds.[29]

Starch Granule Preparation. Starch granules were isolated from soybean seeds using a modification of the amyloplast isolation procedure of Hurkman and Wood.[30] Soybean seeds were imbibed in double-distilled H_2O (ddH_2O) at 25 °C for 12 h in the dark and sown in a Petri dish. After imbibition, cotyledons were chopped with a razor blade and immediately frozen with liquid nitrogen. The cotyledon slices were then homogenized with 10-fold ultrapure water in a Waring blender. This homogenate was quickly filtered through a double layer of nylon mesh (100 meshes). The filtrate was centrifuged at 500*g* for 10 min at 4 °C. The pellets were washed eight times with ultrapure water and were centrifuged at 500*g* for 10 min at 4 °C.

Determination of the Concentration of $HO^{\bullet}$. The production of $HO^{\bullet}$ was evaluated by monitoring the formation of the hydroxylated terephthalate (TA-OH) between TA and $HO^{\bullet}$ as previously described.[31] SSF (1 μM) was incubated in 50 mM Mops buffer (pH 7.0) with 100 mM NaCl, 500 μM TA, and 125 μM ascorbic acid for 24 h at 25 °C. The fluorescence intensity of TA-OH was measured at 326 nm as excitation wavelength (Ex) and at 432 nm as emission wavelength (Em) with a Cary Eclipse fluorescence spectrophotometer (Varian, USA). $HO^{\bullet}$ concentration (nM) in the reaction medium was calculated from the following calibration curve, determined by linear regression (R^2 = 0.999): $Y = 0.107X + 0.033$, where Y is the fluorescence intensity of TA-OH and X is the concentration of $HO^{\bullet}$.

Starch Degradation during Iron Uptake and Release by SSF. To analyze the effect of iron release from holoSSF on the water-soluble starch, 1 mg/mL of the starch was incubated with 1 μM of naturally occurring holoSSF or reconstituted holoSSF with different sizes of iron cores containing 48, 96, 200, and 600 iron/protein shell in 50 mM Mops at pH 7.0 at 25 °C, followed by treatment with different concentrations of ascorbic acid (25, 125, 250, 500, and 1000 μM), respectively. In parallel, to determine the effect of iron uptake by apoSSF on the water-soluble starch, experiments were conducted wherein 1 mg/mL of soluble starch was mixed with 1 μM apoSSF in 50 mM Mops, pH 7.0, followed by aerobic addition of a series of Fe^{2+} solutions at different concentrations (48, 96, 144, 200, and 400 μM). After all of the above solutions were allowed to stand for 24 h, the concentration of the water-soluble starch was analyzed by high-performance size exclusion chromatography (HPSEC) on an HPLC system with refractive index detection, and the column oven temperature was 35 °C. The analytical system was equipped with a Shodex SB 805 HQ HPSEC column (8 mm × 300 mm, separation ranges 100−4,000,000 Da). The mobile phase was sodium nitrate (100 mM), and the flow rate was 0.5 mL/min. Sample and standards, prepared in solution (2 mg/mL), were filtered through a 0.45 μm membrane, and the injection volume was 20 μL.

Effect of $HO^{\bullet}$ Scavenger on Starch Degradation by $HO^{\bullet}$. To determine the effect of $HO^{\bullet}$ scavenger on starch degradation by $HO^{\bullet}$ formed during iron release, water-soluble starch was incubated with 1 μM holoSSF and $HO^{\bullet}$ scavenger (3 mM mannitol or thiourea) in 50 mM Mops, pH 7.0, followed by the addition of ascorbic acid (250 μM). After incubation for 24 h, the concentration of the water-soluble starch was determined as the above-mentioned method.

SEM Analyses of Starch Granules. Intact starch granules were isolated from cotyledons of dried soybean seeds. One milliliter of starch granules (0.1 g/mL) from soybean seeds was incubated with either 1 μM apoSSF and 200 μM $FeSO_4$ for 24 h or with 1 μM holoSSF and 125 μM ascorbic acid for 24 h. Three controls were 0.1 g/mL starch granules, 0.1 g/mL starch granules incubated with 1 μM holoSSF for 24 h, and 0.1 g/mL starch granules incubated with 1 μM

apoSSF and 125 μM ascorbic acid for 24 h. After all samples were lyophilized, the dried starch granules were attached to a SEM stub with silver plate. The mounted samples were spatter-coated with two layers of gold by ion coater (E-1030, Hitachi Ltd.) and were analyzed by scanning electron microscope (S-4500, Hitachi Ltd.).

Determination of the Concentration of Free Iron, Reducing Sugar, and Ascorbic Acid during Seed Germination. Soybean seed germination was carried out by imbibing in ddH_2O at 25 °C in the dark. After germination for 12, 24, 36, and 48 h, respectively, soybean seeds were frozen with liquid nitrogen followed by pulverization into powder. One gram of soybean seed powder was then homogenized with 5 mL of ultrapure water in a Waring blender, vortex-mixed, and centrifuged; the resulting supernatant was collected for the determination of reducing sugar and free iron concentration by the dinitrosalicylic acid (DNS) assay expressed as glucose equivalents[32] and by the ferrozine colorimetric assay[22] expressed as iron μg/g dry seeds, respectively.

Soybean seed powder (20 g) was homogenized with 50 mL of oxalic acid solution (2 mM). The resultant homogenate was quickly filtered through a double layer of nylon mesh (100 mesh), and then the soy milk was transferred to a 50 mL volumetric flask. Ascorbic acid concentration were determined by using the 2,6-dichloroindophenol titrimetric method[33] expressed as μg/g dry seeds.

RESULTS

Subcellular Localization of SSF and Starch Granules. Previous immunoelectron microscopy studies have reported that phytoferritin appears in amyloplasts upon iron citrate treatment of soybean cell culture for 24 h.[34] Ferritin is also mostly localized in the plastids and amyloplasts of infected and uninfected cells of legume nodules.[35] However, no such study on mature soybean seeds has been directly carried out. In the present study information on the subcellular localization of phytoferritin in soybean seeds was obtained with TEM (Figure 1). In agreement with previous observations[34] in mature soybean seeds, SSF molecules are likewise located in amyloplast stroma, and they coexist with starch granules in amyloplasts. Moreover, some SSF molecules stay in an associated state possibly due to low pH in the amyloplast as recently reported.[36]

Different Effects of Iron Uptake and Release by Ferritin on Starch Granules. Both iron uptake and release by SSF occur in amyloplasts,[15,37] but the effect of these two processes on the starch granules is unclear. To shed light on this effect, an in vitro starch granules damage assay was set up, in which the integrity of the starch granules during both iron uptake and release by SSF was determined, respectively. First, the effect of iron uptake by ferritin on the starch granules was analyzed. It was observed that fast iron oxidation was catalyzed by apoSSF (1 μM) upon aerobic addition of 200 Fe^{2+}/protein to the protein at pH 7.0 (Figure 2A). To analyze the effect of this oxidation process on the starch granules, the same experiment was conducted but in the presence of starch granules, followed by the observation with SEM. As shown in Figure 3D, no damage was observed with these starch granules, a result nearly identical to the control (Figure 3A).

Second, the effect of iron release from ferritin on starch granules was determined. Iron release was monitored by the formation of the Fe^{2+}–ferrozine complex at 562 nm upon treatment of holoSSF (0.2 μM) in 50 mM Mops, pH 7.0, with ascorbic acid (125 μM) as recently described[22,28] (Figure 2B). Compared to the iron oxidation, the iron release from holoferritin induced by ascorbic acid is a much slower process, consistent with previous observations.[1,22,28] Subsequently, the same experiment was carried out but in the presence of starch granules, followed by the observation with SEM. It was found

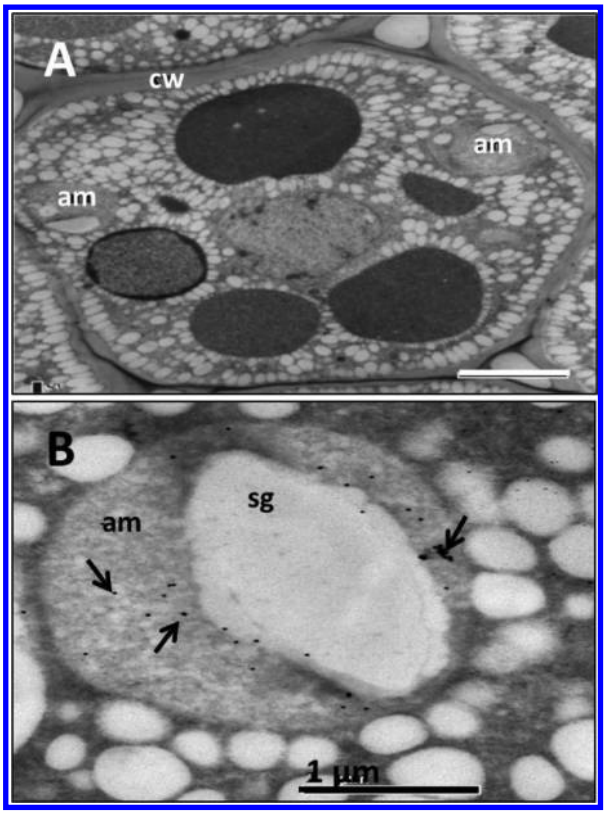

Figure 1. TEM images of SSF subcellular localization in soybean seeds. Soybean seed cell sections were treated with polyclonal antibody to SSF followed by IgG-conjugated 10 nm colloidal gold (arrows). Gold particles are observed only in amyloplasts. cw, cell wall; am, amyloplast; sg, starch granule. Bars are 5 and 1 μm in panels A and B, respectively.

that the starch granules were dramatically damaged during this process (Figure 3E). In contrast, starch granules incubated with apoferritin with ascorbic acid and holoferritin were kept intact (Figure 3B,C). These results indicated that these two processes have markedly different influences on the integrity of the starch granules.

Hydroxyl Radical Detection. It has been established that hydroxyl radicals can cause oxidative scission of various polysaccharides such as chitosan, pectin, and starch.[38,39] To elucidate the reason for the above observed different effects of iron uptake and release by ferritin on the starch granules, the formation of $HO^{\bullet}$ was analyzed during iron uptake and release according to a reported method where terephthalate (TA) was used as the $HO^{\bullet}$ trapping reagent.[31] The concentration of $HO^{\bullet}$ was determined as TA-$HO^{\bullet}$ adduct during these two processes, respectively. As shown in Figure 2C, the concentration of TA-$HO^{\bullet}$ adduct reached 317.4 ± 11.3 nM during iron release from holoSSF (1 μM) induced by 125 μM ascorbic acid, which is about 14-fold larger than that generated by iron uptake at 200 Fe^{2+}/protein iron flux into the protein at pH 7.0 (23.1 ± 4.5 nM). These results suggested that much more hydroxyl radical was produced during the iron release as compared to the iron uptake, which could be responsible for the above observed starch damage.

In parallel, the time curves of the TA-$HO^{\bullet}$ adduct formation for these two processes were obtained, which are given in Figure 2D. The adduct concentration linearly increased with time in the range of 330 min during the iron release, reaching

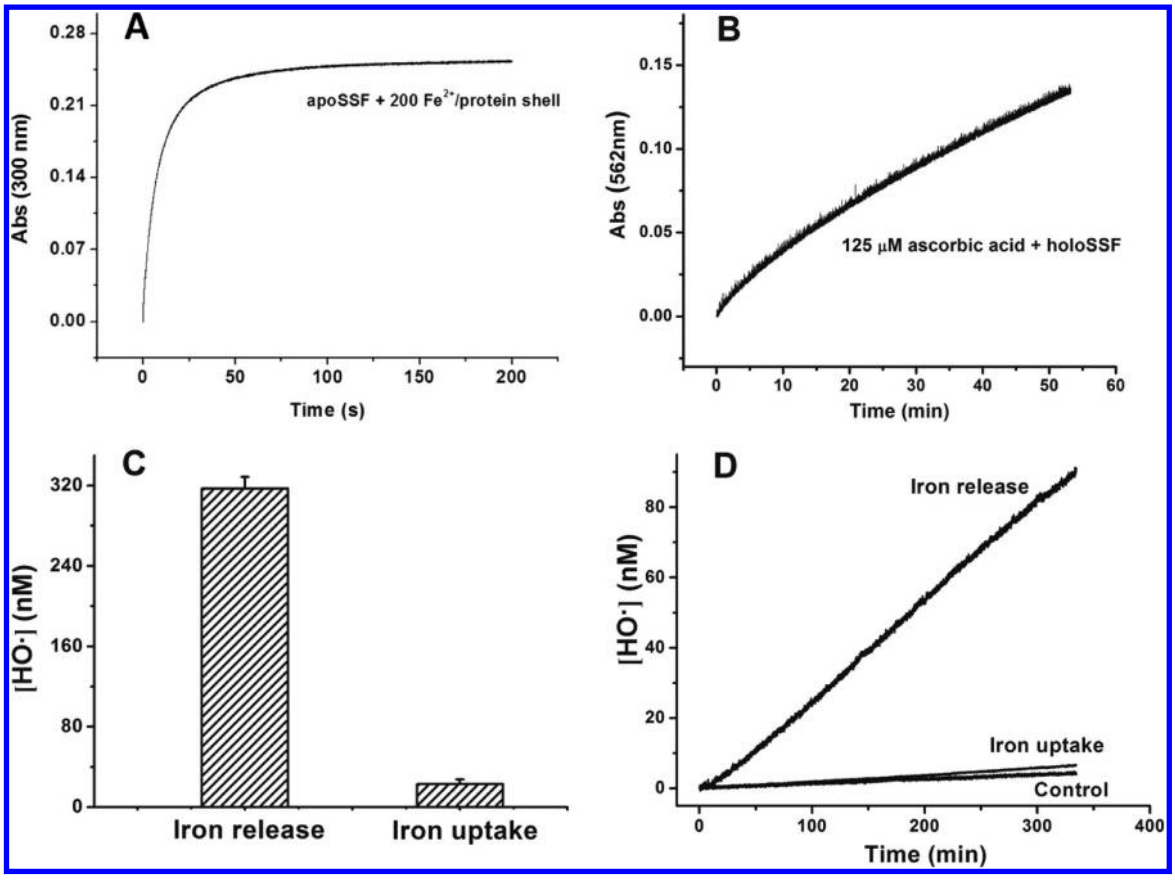

Figure 2. Kinetic curves of Fe^{2+} oxidation and iron release by soybean seed ferritin and hydroxyl radical generated during iron uptake and release processes. (A) Fe^{2+} oxidation by O_2 in the presence of apoSSF. Conditions: final [apoferritin] = 0.5 μM, in 50 mM Mops, pH 7.0, [$FeSO_4$] = 100 μM, 25 °C. (B) Iron release from holoSSF induced by ascorbic acid. Conditions: 0.2 μM holoSSF, 125 μM ascorbic acid, 50 mM Mops, pH 7.0, 500 μM ferrozine, 25 °C. (C) Determination of $HO^{\bullet}$ concentration in 12 h. Vertical bars represent the standard errors from the means of three independent experiments. Conditions: 1.0 μM holoSSF, 50 mM Mops (pH 7.0), 1 mM TA, and 125 μM ascorbic acid. Values are means ± SE (n = 3). (D) Kinetic curves of $HO^{\bullet}$ generated during iron uptake and release by SSF. Conditions: 1 μM holoSSF, 1 μM apoSSF, 125 μM ascorbic acid, 50 mM Mops, pH 7.0, 500 μM ferrozine, 25 °C.

90 nM at 330 min. In contrast, the kinetic curve of the radical formation for the iron deposition nearly overlapped with that of the control, and the concentration of this adduct is only ~6 nM at 330 min.

Water-Soluble Starch Degradation. The above results showed that $HO^{\bullet}$ was produced mainly during the iron release process, whereas such radical was hardly formed during iron uptake by SSF. If this is the case, we would expect that starch hydrolysis occurs during the iron release process due to $HO^{\bullet}$ attack as previously reported.[38,39] To confirm this idea, the content of starch hydrolysis was analyzed at different iron deposition and release experimental conditions, respectively. To make the hydrolysis reaction easily detected, water-soluble starch was used instead of starch granules. As expected, the content of water-soluble starch decreased by only approximately 8% upon increase of the ratio of Fe^{2+} to apoSSF from 0 to 400/1 (Figure 3F). In contrast, the starch was greatly hydrolyzed during the iron relase from holoSSF, and the concentration of a reducing reagent, ascorbic acid, has a large effect on the hydrolysis of the water-soluble starch during iron release (Figure 3G). The degree of the starch hydrolysis rapidly increased with the increase ascorbic acid concentration, reaching its maximum at 500 μM ascorbic acid, beyond which no further hydrolysis was observed (Figure 3G).

In parallel, the damage extent of the starch granules from soybean seed was analyzed by scanning electron microscope (SEM). Consistent with the above observation with the water-soluble starch, the starch granules were almost not damaged during iron oxidation even upon incubation with apoSSF (1 μM) treated aerobically with 400 Fe^{2+}/protein (Figure 4B), a result nearly the same as the control (Figure 4A). By comparison, the starch granule degradation occurs seriously after the incubation with holoSSF in the presence of ascorbic acid (500 μM) (Figure 4C), agreeing with the above observation (Figure 3G). Such degradation happened to a much larger extent when 1000 μM ascorbic acid was used (Figure 4D). This observation is different from the above result obtained with water-soluble starch (Figure 3G), reflecting the different reactivities of both water-soluble and -insoluble starch.

Measurements of Fe^{2+}/O_2 Stoichiometry and H_2O_2 during Iron Oxidation. Hydroxyl radical was hardly produced during iron uptake by apoSSF. To elucidate the reason for this observation, measurements of Fe^{2+}/O_2 stoichiometry were performed during iron oxidation in the presence of apoSSF using electrode oximetry. Meanwhile, the formation of H_2O_2 was directly probed by the addition of catalase, an enzyme that specifically catalyzes the decomposition of hydrogen peroxide into water and dioxygen as shown in eq 1.

$$2H_2O_2 \rightarrow 2H_2O + O_2 \quad (1)$$

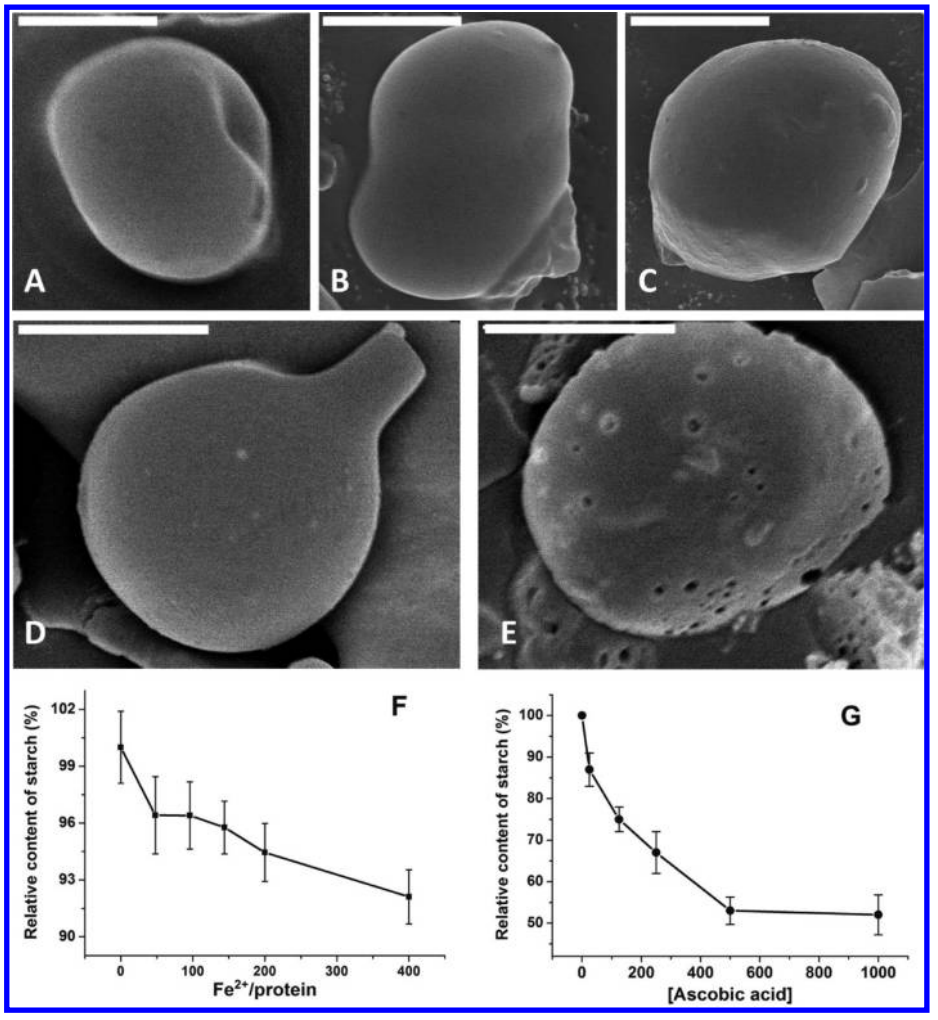

Figure 3. (A–E) Scanning electron micrographs of soybean starch granules: (A) 0.1 g/mL starch granules alone; (B) 0.1 g/mL starch granules with 1 μM apoSSF and 125 μM ascorbic acid in 50 mM MOPS pH 7.0; (C) 0.1 g/mL starch granules with 1 μM holoSSF in 50 mM MOPS pH 7.0; (D) 0.1 g/mL starch granules in the presence of apoSSF (1 μM), where 200 μM $FeSO_4$ was aerobically added; (E) 0.1 g/mL starch granules incubated with 1 μM holoSSF and 125 μM ascorbic acid. (F, G) Starch degradation during iron deposition and release: (F) during iron deposition into apoSSF (conditions: 1 mg/mL soluble starch, 1 μM apoSSF, 50 mM Mops (pH 7.0), [$FeSO_4$] = 48, 96, 144, 200, and 400 μM); (G) during iron release from holoSSF (conditions: 1 mg/mL soluble starch, 1 μM holoSSF, 50 mM Mops (pH 7.0), [ascorbic acid] = 25, 125, 250, 500, and 1000 μM). Bars are 5 μm. Values are means ± SE (n = 3).

When 48 Fe^{2+}/protein shell was added to 1 μM apoSSF, a stoichiometry of ~4Fe^{2+}/O_2 was observed (Figure 5). This value resulted from the combination of detoxification and ferroxidase reactions as recently found.[13,28] Indeed, no oxygen evolution was observed after catalase was injected into the solution (Figure 5), indicating that H_2O_2 produced by the ferroxidase reaction was consumed by the detoxification reaction.[13]

Effect of Hydroxyl Radical Scavengers and H_2O_2 on Starch Hydrolysis. Starch degradation during iron release might come from hydroxyl radical. To confirm this idea, several experiments were performed wherein two hydroxyl radical scavengers and H_2O_2 were added to the mixture containing water-soluble starch, holoSSF, and ascorbic acid, respectively. Figure 6 summarizes the effects of 3 mM thiourea and mannitol (which are known to be effective $HO^•$ scavengers) on the hydrolysis extent of the water-soluble starch. The starch was hydrolyzed by ~32% in the absence of hydroxyl radical scavenger. In contrast, the hydrolysis rate of the water-soluble starch is diminished by 15% in the presence of mannitol and by 17% in the presence of thiourea. Furthermore, the addition of 3 mM of H_2O_2 to the reaction mixture enhances the hydrolysis rate of the water-soluble starch by a factor of 2, which reached ~70%. Thus, these results indicated that hydroxyl radicals are mainly responsible for the starch degradation, which stemmed from the Fenton reaction occurring during iron release from holoSSF.

Iron Release from HoloSSF. The starch hydrolysis during iron release might be derived from the iron-catalyzed $HO^•$. To confirm this idea, one important reductant of Fenton reaction, ferrous ion, was quantitatively analyzed upon treatment of holoSSF with various amounts of ascorbic acid by the formation of the Fe^{2+}–ferrozine complex at 562 nm as previously described,[21] respectively, and at the same time, its release kinetic was also monitored. As shown in Figure 7A, the amount of released ferrous ions also increased as a function of the concentration of ascorbic acid. On the other hand, the rate of iron release increased linearly with an increase in the concentration of ascorbic acid (Figure 7B), indicating that the iron release is first order with respect to ascorbic acid. These results imply that diffusion of ascorbic acid into the ferritin shell may be the first step of iron release. These results are consistent

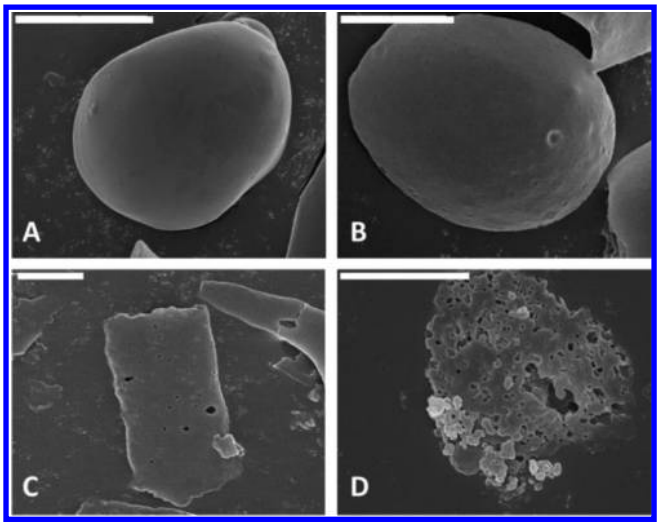

Figure 4. Effect of iron uptake and release by SSF on SEM of soybean starch granules: (A) 0.1 g/mL starch granules alone; (B) 0.1 g/mL starch granules + 1.0 μM apoSSF + 400 μM $FeSO_4$; (C) 0.1 g/mL starch granules + 1.0 μM holoSSF + 500 μM ascorbic acid; (D) 0.1 g/mL starch granules + 1.0 μM holoSSF + 1000 μM ascorbic acid. Bars are 5 μm.

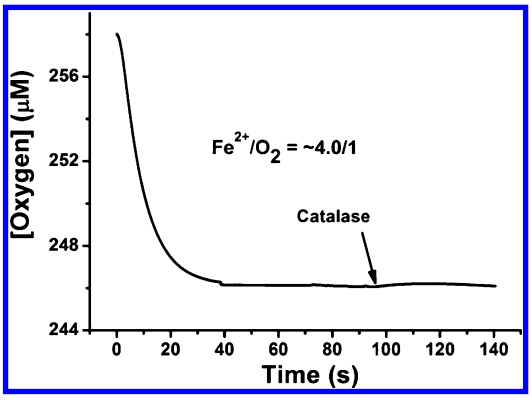

Figure 5. Fe^{2+}/O_2 stoichiometry and H_2O_2 measurement by electrode oximetry upon aerobic addition of ferrous ions to apoSSF. Conditions: [apoSSF] = 1.0 μM in 0.1 M Mops and 50 mM NaCl (pH 7.0), [Fe^{2+}] = 48 μM, 25 °C.

with the above observation that the degree of starch granule degradation during iron release increased with increasing concentration of ascorbic acid (Figure 4).

Determination of the Concentration of Reducing Sugar, Ascorbic Acid, Ferrous Ions, and Hydroxyl Radical during Soybean Seed Germination. The above results demonstrated that ferrous ions released from holoSSF in the presence of ascorbic acid facilitate starch hydrolysis in vitro. To elucidate whether these processes likewise occur in vivo, the concentration of reducing sugar, ascorbic acid, ferrous ions, and HO• during soybean seed germination was investigated, respectively, as a function of germination time. As shown in Figure 8A, the concentration of reducing sugar increased with an increase in germination time over the range of 48 h. At the same time, increased ascorbic acid concentration was also observed, which is the same as in previous studies.[40,41] Associated with this increase is the increase in the concentration of free iron ions and HO• during soybean seed germination (Figure 8B). Thus, these four parameters are closely related with each other, consistent with the in vitro

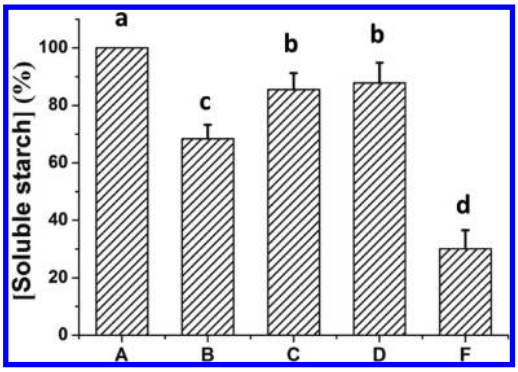

Figure 6. Effect of HO• scavengers and hydrogen peroxide on soluble starch hydrolysis during iron release: (A) starch alone; (B) starch + holoferrtin + ascorbic acid; (C) starch + holoferrtin + ascorbic acid + mannitol; (D) starch + holoferrtin + ascorbic acid + thiourea; (E) starch + holoferrtin + ascorbic acid + H_2O_2. Conditions: 1.0 mg/mL soluble starch, 1.0 μM holoSSF, 50 mM Mops (pH 7.0), 250 μM ascorbic acid, 3 mM mannitol, 3 mM thiourea, 3 mM H_2O_2. Values are means ± SE (n = 3); means with different lower case letters are significantly different at α = 0.5 using Duncan's multiple-range test.

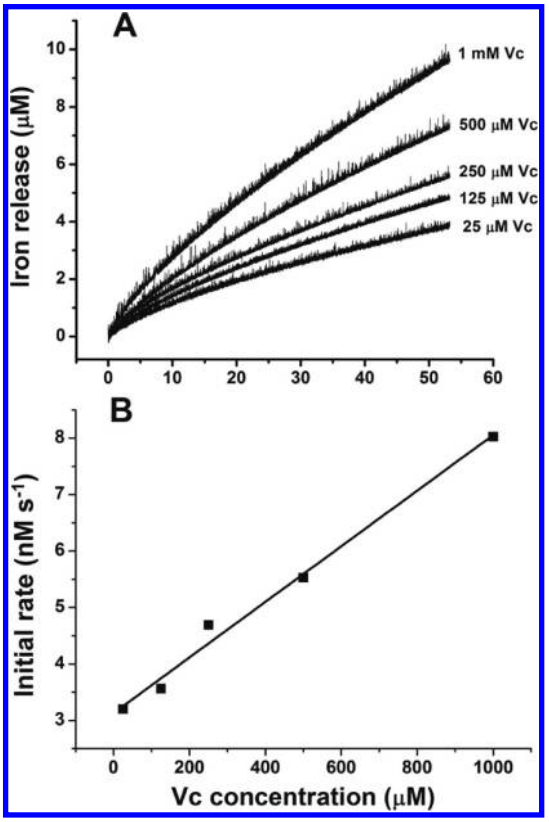

Figure 7. Iron release from holoSSF induced by different amounts of ascorbic acid: (A) kinetic curves of iron release; (B) correlation of the initial rate of iron release with ascorbic acid concentration. Conditions: [holoSSF] = 0.2 μM in 50 mM Mops, pH 7.0, [ascorbic acid] = 25, 125, 250, 500, and 1000 μM, 500 μM ferrozine, 25 °C.

conclusion that iron release from holoSSF induced by ascorbic acid might result in the degradation of starch granules.

DISCUSSION

Accompanied by the formation of legume seeds, iron uptake by apoferritin results in the formation of holoferritin, which was found to occur in amylopalst.[15,37] Similarly, in the seedling

dx.doi.org/10.1021/jf402826p | J. Agric. Food Chem. 2013, 61, 8215−8223

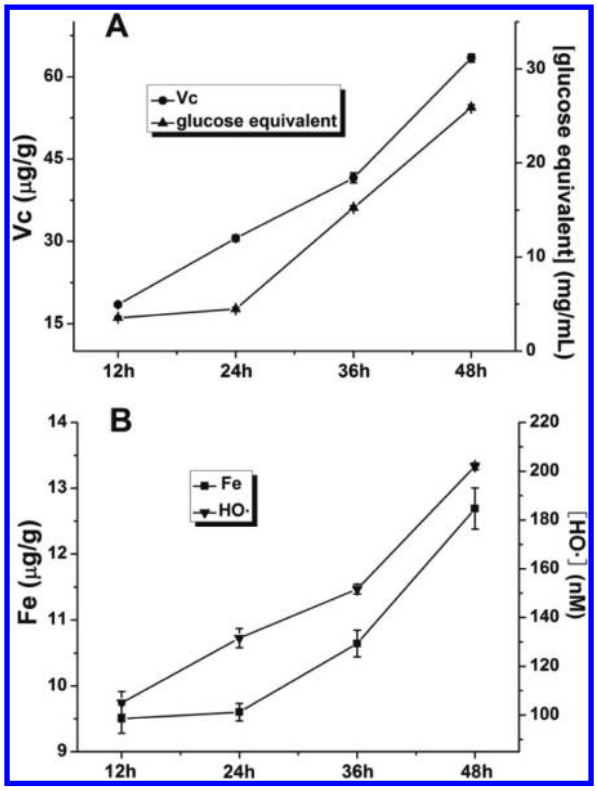

Figure 8. Content of Fe, ascorbic acid, hydroxyl radicals, and reducing sugar in germinated soybean seeds as a function of germination time. Values are means ± SE (n = 3).

stage, ferritin iron release likewise happens in the amyloplast, and these released irons were believed to meet the demand of various key physiological processes, such as electron transfer and DNA synthesis.[15] However, the effect of these two processes on starch granules remains unknown. The present study demonstrated for the first time that the transit of iron into and out of the ferritin cavity has different effects on the integrity of starch granules; namely, iron uptake by plant ferritin causes no damage to starch granules, whereas iron release from plant ferritin greatly facilitates starch hydrolysis (Figures 3D,E and 4). Such difference is derived from their different strategies to regulate HO$^\bullet$ chemistry. For example, HO$^\bullet$ was significantly generated upon aerobic addition of ascorbic acid to holoferritin (Figure 2C,D). In contrast, almost no HO$^\bullet$ was detected during iron uptake by apoSSF regardless of iron concentration (Figure 2C,D), consistent with our recent finding.[42]

The reason for the inhibition of hydroxyl radical formation during iron uptake might be derived from tightly controlled iron chemistry by SSF. Indeed, the electrode oximetry results showed that the Fe^{2+}/O_2 stoichiometry in the presence of apoSSF was about 4:1 (Figure 5). The stoichiometry of the complete reduction of oxygen to water is 4:1 Fe^{2+}/O_2, which is a sequential four-electron transfer, that is, $O_2 \rightarrow O_2^{\bullet-} \rightarrow H_2O_2 \rightarrow HO^\bullet \rightarrow H_2O$. Therefore, in the presence of apoSSF, O_2 was completely reduced into water, preventing the formation of H_2O_2, which can react with unreacted ferrous ions to produce HO$^\bullet$ through Fenton reaction. Consistent with this conclusion, our recent studies showed that heteropolymeric soybean seed ferritin can protect DNA from oxidative damage by inhibiting the Fenton reaction.[42] Moreover, H-type ferritin, HuHF, was found to also have such a function to attenuate the formation of HO$^\bullet$.[13] Thus, it appears that both animal and plant ferrritins have developed the same strategy to cope with HO$^\bullet$.

In contrast, there is a significant amount of HO$^\bullet$ generated during iron release from holoferritin as shown in Figure 2C,D. This should come as no surprise because free ferrous ions can trigger the generation of highly reactive oxygen species (ROS) via the iron-catalyzed Haber−Weiss reactions.[3,4] Consistent with this idea, the HO$^\bullet$ scavengers such as thiourea and mannitol significantly inhibited starch hydrolysis by ∼15%, whereas hydrogen peroxide increased such hydrolysis >2-fold (Figure 6). These results demonstrated that free ferrous ions released from holoferritin facilitated the formation of hydroxyl radicals possibly through the Fenton reaction.

What advantage might Fe^{2+}-induced HO$^\bullet$ formation during the iron release render to the cells during seedling germination and growth? The answer to this question may lie in the experimental results of the starch hydrolysis. The content of water-soluble starch decreased with the increasing concentration of ascorbic acid, a naturally occurring reducing reagent in legume seeds (Figure 3G). In support of this observation, a SEM image showed that the starch granules were pronouncedly damaged during the iron release process, and such damage increased in a dose-dependent manner (Figure 4). SEM analyses also revealed that starch granules are attacked by HO$^\bullet$, producing many "pinholes", which are randomly distributed on the starch granules, indicative of no selectivity on the starch granules (Figures 3 and 4). In contrast, starch degradation by enzymes can be divided into two types. One is that lenticular granules are enzymatically attacked around the equatorial groove, showing a relatively high selectivity;[43] the other is that starch granules are enzymatically hydrolyzed in "pinholes" or "scratches".[44,45] The latter pattern seems to exhibit much lower selectivity, and the pores are very similar to the case of hydroxyl radical attack reported in this study. Similar to starch degradation induced by amylase,[46] HO$^\bullet$-induced starch degradation consequently produces glucose and other reducing sugars (Figures 6 and 8A), and thus this process may favor various synthesis reactions at the seedling stage. In agreement with the above proposal, it was observed that with an increase in germination time, the content of ascorbic acid increased over the range of 48 h (Figure 8A). Related to such an increase is an increase in the concentration of reducing sugar (Figure 8A). Thus, it is possible that the increase in the concentration of ascorbic acid facilitates iron release from holoferritin (Figure 7) because ∼90% of the total iron is stored in ferritin.[2,47] As expected, free iron concentration increased as a function of germination time (Figure 8B), and these released ferrous ions could trigger the generation of hydroxyl radicals through iron-catalyzed Haber−Weiss reactions, finally leading to the generation of reducing sugars.

Different from animal proteins, proteins in plants usually have evolved multiple functions for adaptation to these environmental stresses. The present and previous findings raise the possibility that phytoferritin in legume seeds has at least three functions. One is iron storage within their inner cavity for seedling development.[2,15] During this iron storage process, starch granules are well protected from oxidative damage (Figure 3D). The second function is to release stored iron from its inner cavity to the bulk solution to meet the needs of different iron-required physiological processes such as nitrogen fixation and electron transfer.[15] The third is that hydroxyl radicals produced during iron release from holoferritin may help hydrolyze the starch granules during seed

germination. This pathway might coexist with other pathways of starch granule hydrolysis by enzymes such as α-amylase, β-amylase, and α-glucosidase.[46,48] Throughout their life cycle, plants often experience various stresses such as drought, cold, light intensity, and pathogen attack. All of these stresses can transiently lead to the generation of ROS, which cause the damage of the above enzymes involved in the starch granules hydrolysis. By that time, the ferritin-regulated starch hydrolysis could play a more important role.

In summary, the present work demonstrates that iron uptake and release by phytoferritin have different effects on the integrity of the starch granules that were previously unrecognized. During iron uptake, no damage was observed with the granules because almost no $HO^{\bullet}$ was produced during this process. In contrast, starch granules were greatly damaged during iron release from holoferritin induced by ascorbic acid. This is mainly due to the generation of a significant amount of $HO^{\bullet}$ through Fenton reaction during iron release from holoferritin. The hydrolysis of starch granules might be beneficial to iron utilization in various physiological processes such as protein and DNA synthesis during seed germination. These findings advance our understanding of the fact that ferritin and starch granules coexist in the amyloplast of legume seeds.

AUTHOR INFORMATION

Corresponding Author

*(G.Z.) Phone: +86-10-62738737. Fax: +86-10-62738737. E-mail: gzhao@cau.edu.cn.

Funding

This work was supported by the National Natural Science Foundation of China (31271826) and the National Science and Technology Support Program (2011BAD23B04).

Notes

The authors declare no competing financial interest.

ABBREVIATIONS USED

EP, extension peptide; SSF, soybean seed ferritin; $HO^{\bullet}$, hydroxyl radical; TEM, transition electron microscope; SEM, scanning electron microscope; TA-OH, hydroxylated terephthalate

REFERENCES

(1) Harrison, P. M.; Arosio, P. The ferritins: molecular properties, iron storage function and cellular regulation. *Biochim. Biophys. Acta* **1996**, *1275*, 161−203.

(2) Theil, E. C. Iron, ferritin, and nutrition. *Annu. Rev. Nutr.* **2004**, *24*, 327−343.

(3) Haber, F.; Weiss, J. The catalytic decomposition of hydrogen peroxide by iron salts. *Proc. R. Soc. London A* **1934**, *147*, 332−351.

(4) Kehrer, J. P. The Haber-Weiss reaction and mechanisms of toxicity. *Toxicology* **2000**, *149*, 43−50.

(5) Halliwell, B.; Gutteridge, J. M. Oxygen toxicity, oxygen radicals, transition metals and disease. *Biochem. J.* **1984**, *219*, 1−14.

(6) McCord, J. M. Iron, free radicals, and oxidative injury. *Semin. Hematol.* **1998**, *35*, 5−12.

(7) Schopfer, P. Hydroxyl radical-induced cell-wall loosening in vitro and in vivo: implications for the control of elongation growth. *Plant J.* **2001**, *28*, 679−688.

(8) Schopfer, P.; Plachy, C.; Frahry, G. ROI production by germinating seeds represents an active, developmentally controlled physiological function, presumably for protecting the emerging seedling against attack by pathogens. *Plant Physiol.* **2001**, *125*, 1591−1602.

(9) Arosio, P.; Ingrassia, R.; Cavadini, P. Ferritins: a family of molecules for iron storage, antioxidation and more. *Biochim. Biophys. Acta* **2008**, *1790*, 589−599.

(10) Crichton, R. R.; Herbas, A.; Chavez-Alba, O.; Roland, F. Identification of catalytic residues involved in iron uptake by L-chain ferritins. *J. Biol. Inorg. Chem.* **1996**, *1*, 567−574.

(11) Bou-Abdallah, F. The iron redox and hydrolysis chemistry of the ferritins. *Biochim. Biophys. Acta* **2010**, *1800*, 719−731.

(12) Chasteen, N. D.; Harrison, P. M. Mineralization in ferritin: an efficient means of iron storage. *J. Struct. Biol.* **1999**, *126*, 182−194.

(13) Zhao, G.; Arosio, P.; Chasteen, N. D. Iron(II) and hydrogen peroxide detoxification by human H-chain ferritin. An EPR spin-trapping study. *Biochemistry* **2006**, *45*, 3429−3436.

(14) Zhao, G. Phytoferritin and its implications for human health and nutrition. *Biochim. Biophys. Acta* **2010**, *1800*, 815−823.

(15) Briat, J. F.; Lobréaux, S.; Grignon, N.; Vansuyt, G. Regulation of plant ferritin synthesis: how and why. *Cell. Mol. Life Sci.* **1999**, *56*, 155−166.

(16) Seckbach, J. J. Ferreting out the secrets of plant ferritin: a review. *J. Plant Nutr.* **1982**, *5*, 369−394.

(17) Proudhon, D.; Briat, J. F.; Lescure, A. M. Iron induction of ferritin synthesis in soybean cell suspensions. *Plant Physiol.* **1989**, *90*, 586−590.

(18) Grady, J. K.; Chen, Y.; Chasteen, N. D.; Harris, D. C. Hydroxyl radical production during oxidative deposition of iron in ferritin. *J. Biol. Chem.* **1989**, *264*, 20224−20229.

(19) Van Eden, M. E.; Aust, S. D. The consequences of hydroxyl radical formation on the stoichiometry and kinetics of ferrous iron oxidation by human apoferritin. *Free Radical Biol. Med.* **2001**, *31*, 1007−1017.

(20) Laulhere, J. P.; Laboure, A. M.; Briat, J. F. Mechanism of the transition from plant ferritin to phytosiderin. *J. Biol. Chem.* **1989**, *264*, 3629−3635.

(21) Lobréaux, S.; Briat, J. F. Ferritin accumulation and degradation in different organs of pea (*Pisum sativum*) during development. *Biochem. J.* **1991**, *274*, 601−606.

(22) Fu, X.; Deng, J.; Yang, H.; Masuda, T.; Goto, F.; Yoshihara, T.; Zhao, G. A novel EP-involved pathway for iron release from soya bean seed ferritin. *Biochem. J.* **2010**, *427*, 313−321.

(23) Bauminger, E. R.; Harrison, P. M.; Hechel, D.; Nowik, I.; Treffry, A. Mössbauer spectroscopic investigation of structure−function relations in ferritins. *Biochim. Biophys. Acta* **1991**, *1118*, 48−58.

(24) Treffry, A.; Hirzmann, J.; Yewdall, S. J.; Harrison, P. M. Mechanism of catalysis of Fe(II) oxidation by ferritin H-chains. *FEBS Lett.* **1992**, *302*, 108−112.

(25) Bendayan, M.; Zollinger, M. Ultrastructural localization of antigenic sites on osmium-fixed tissues applying the protein A-gold technique. *J. Histochem. Cytochem.* **1983**, *31*, 101−109.

(26) Date, Y.; Kojima, M.; Hosoda, H.; Sawaguchi, A.; Mondal, M. S.; Suganuma, T.; Matsukura, S.; Kangawa, K.; Nakazato, M. Ghrelin, a novel growth hormone-releasing acylated peptide, is synthesized in a distinct endocrine cell type in the gastrointestinal tracts of rats and humans. *Endocrinology* **2000**, *141*, 4255−4261.

(27) Li, C.; Qi, X.; Li, M.; Zhao, G.; Hu, X. Phosphate facilitates Fe(II) oxidative deposition in pea seed (*Pisum sativum*) ferritin. *Biochimie* **2009**, *91*, 1475−1481.

(28) Deng, J.; Cheng, J.; Liao, X.; Zhang, T.; Leng, X.; Zhao, G. Comparative study on iron release from soybean (*Glycine max*) seed ferritin induced by anthocyanins and ascorbate. *J. Agric. Food Chem.* **2010**, *58*, 635−641.

(29) Zhao, G.; Bou-Abdallah, F.; Arosio, P.; Levi, S.; Janus-Chandler, C.; Chasteen, N. D. Multiple pathways for mineral core formation in mammalian apoferritin: the role of hydrogen peroxide. *Biochemistry* **2003**, *42*, 3142−3150.

(30) Hurkman, W. J.; Wood, D. F. High temperature during grain fill alters the morphology of protein and starch deposits in the starchy endosperm cells of developing wheat (*Triticum aestivum* L.) grain. *J. Agric. Food Chem.* **2011**, *59*, 4938−4946.

(31) Freinbichler, W.; Colivicchi, M. A.; Fattori, M.; Ballini, C.; Tipton, K. F.; Linert, W.; Della Corte, L. Validation of a robust and sensitive method for detecting hydroxyl radical formation together with evoked neurotransmitter release in brain microdialysis. *J. Neurochem.* **2008**, *105*, 738−749.
(32) Miller, G. L. Use of dinitrosalicylic acid reagent for the determination of reducing sugars. *Anal. Chem.* **1959**, *31*, 426−428.
(33) Dadali, G.; Özbek, B. Kinetic thermal degradation of vitamin C during microwave drying of okra and spinach. *Int. J. Food Sci. Nutr.* **2009**, *60*, 21−31.
(34) Lescure, A. M.; Proudhon, D.; Pesey, H.; Ragland, M.; Theil, E. C.; Briat, J. F. Ferritin gene transcription is regulated by iron in soybean cell cultures. *Proc. Natl. Acad. Sci. U.S.A.* **1991**, *88*, 8222−8226.
(35) McCullough, A. J.; Kangasjarvi, J.; Gengenbach, B. G.; Jones, R. J. Plastid DNA in developing maize endosperm: genome structure, methylation, and transcript accumulation patterns. *Plant Physiol.* **1992**, *100*, 958−964.
(36) Yang, H.; Fu, X.; Li, M.; Leng, X.; Chen, B.; Zhao, G. Protein association and dissociation regulated by extension peptide: a mode for iron control by phytoferritin in seeds. *Plant Physiol.* **2010**, *154*, 1481−1491.
(37) Waldo, G. S.; Wright, E.; Whang, Z. H.; Briat, J. F.; Theil, E. C.; Sayers, D. E. Formation of the ferritin iron mineral occurs in plastids. *Plant Physiol.* **1995**, *109*, 797−802.
(38) Fry, S. C. Oxidative scission of plant cell wall polysaccharides by ascorbate-induced hydroxyl radicals. *Biochem. J.* **1998**, *332*, 507−515.
(39) Czechowska-Biskup, R.; Rokita, B.; Lotfy, S.; Ulanski, P.; Rosiak, J. M. Degradation of chitosan and starch by 360-kHz ultrasound. *Carbohydr. Polym.* **2005**, *60*, 175−184.
(40) Wheeler, G. L.; Jones, M. A.; Smirnoff, N. The biosynthetic pathway of vitamin C in higher plants. *Nature* **1998**, *393*, 365−369.
(41) Garnczarska, M.; Wojtyla, Ł. Ascorbate and glutathione metabolism in embryo axes and cotyledons of germinating lupine seeds. *Biol. Plant.* **2008**, *52*, 681−686.
(42) Liao, X.; Lv, C.; Zhang, X.; Masuda, T.; Li, M.; Zhao, G. A novel strategy of natural plant ferritin to protect DNA from oxidative damage during iron oxidation. *Free Radical Biol. Med.* **2012**, *53*, 375−382.
(43) Sun, Z.; Henson, C. A. Degradation of native starch granules by barley α-glucosidases. *Plant Physiol.* **1990**, *94*, 320−327.
(44) Zhang, B.; Dhital, S.; Gidley, M. J. Synergistic and antagonistic effects of α-amylase and amyloglucosidase on starch digestion. *Biomacromolecules* **2013**, *14*, 1945−1954.
(45) Lee, T. T.; Huag, Y. F.; Chiang, C. C.; Chung, T. K.; Chiou, P. W.; Yu, B. Starch characteristics and their influences on in vitro and pig prececal starch digestion. *J. Agric. Food Chem.* **2011**, *59*, 7353−7359.
(46) Stanley, D.; Rejzek, M.; Naested, H.; Smedley, M.; Otero, S.; Fahy, B.; Thorpe, F.; Nash, R. J.; Harwood, W.; Svensson, B.; Denyer, K.; Field, R. A.; Smith, A. M. The role of α-glucosidase in germinating barley grains. *Plant Physiol.* **2011**, *155*, 932−943.
(47) Ambe, S.; Ambe, F.; Nozaki, T. Mössbauer study of iron in soybean seeds. *J. Agric. Food Chem.* **1987**, *35*, 292−296.
(48) Bamforth, C. W. Current perspectives on the role of enzymes in brewing. *J. Cereal Sci.* **2009**, *50*, 353−357.